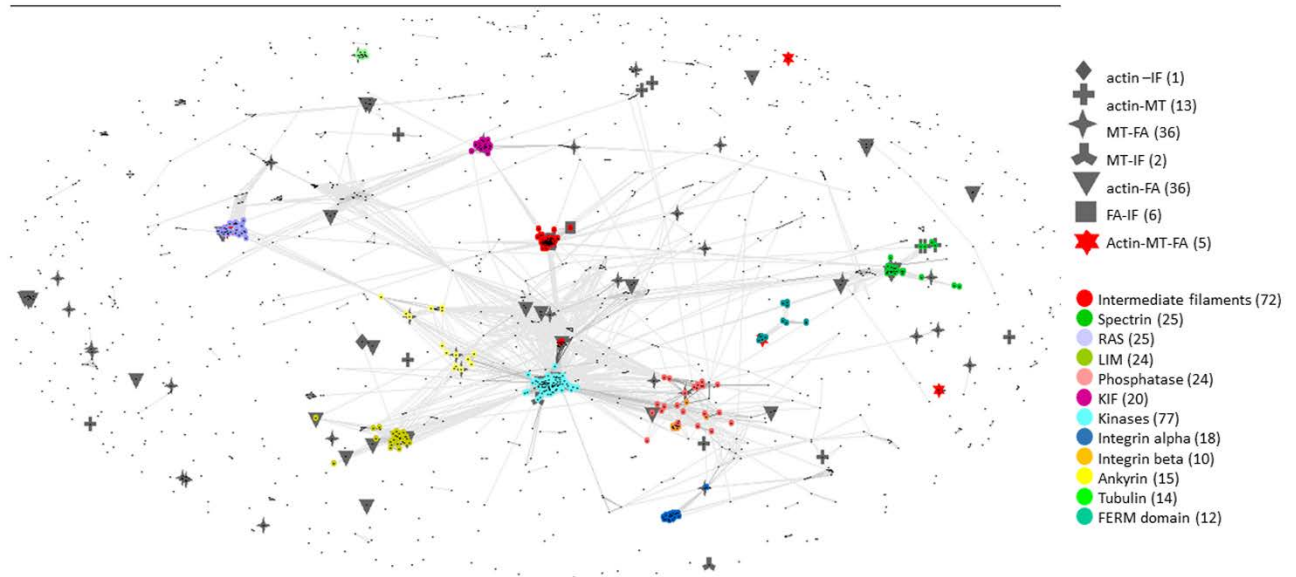
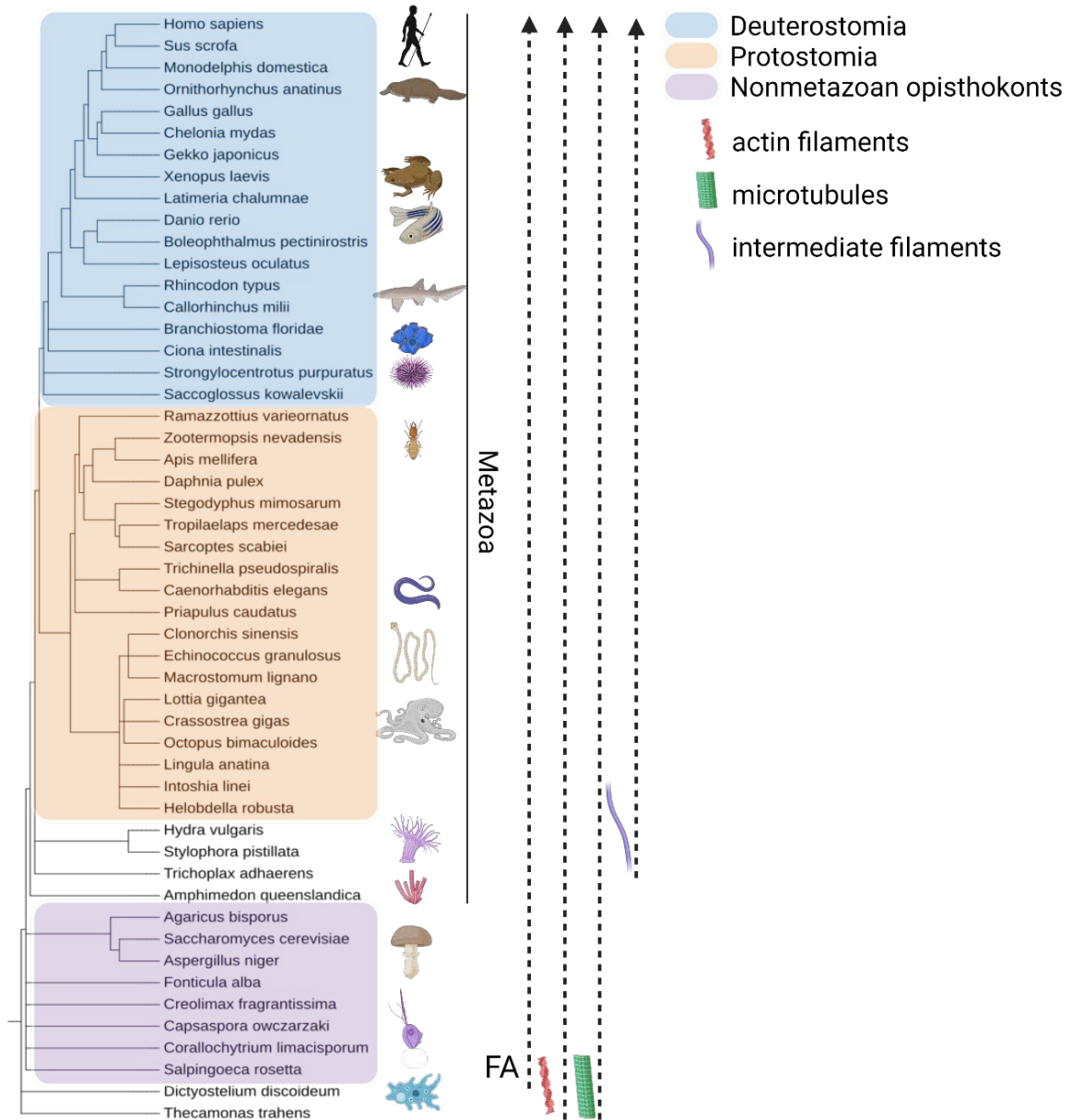


## Supplementary Materials



**Figure S1. CLANS clustering of human cytoskeleton proteins.** Different protein families are assigned with different colors, while intersection proteins are depicted with different symbols.



**Figure S2.** Phylogenetic tree made by PhyloT tool containing organismal dataset used in this study. Presence of different cytoskeletal components in these organisms is designated on the right.

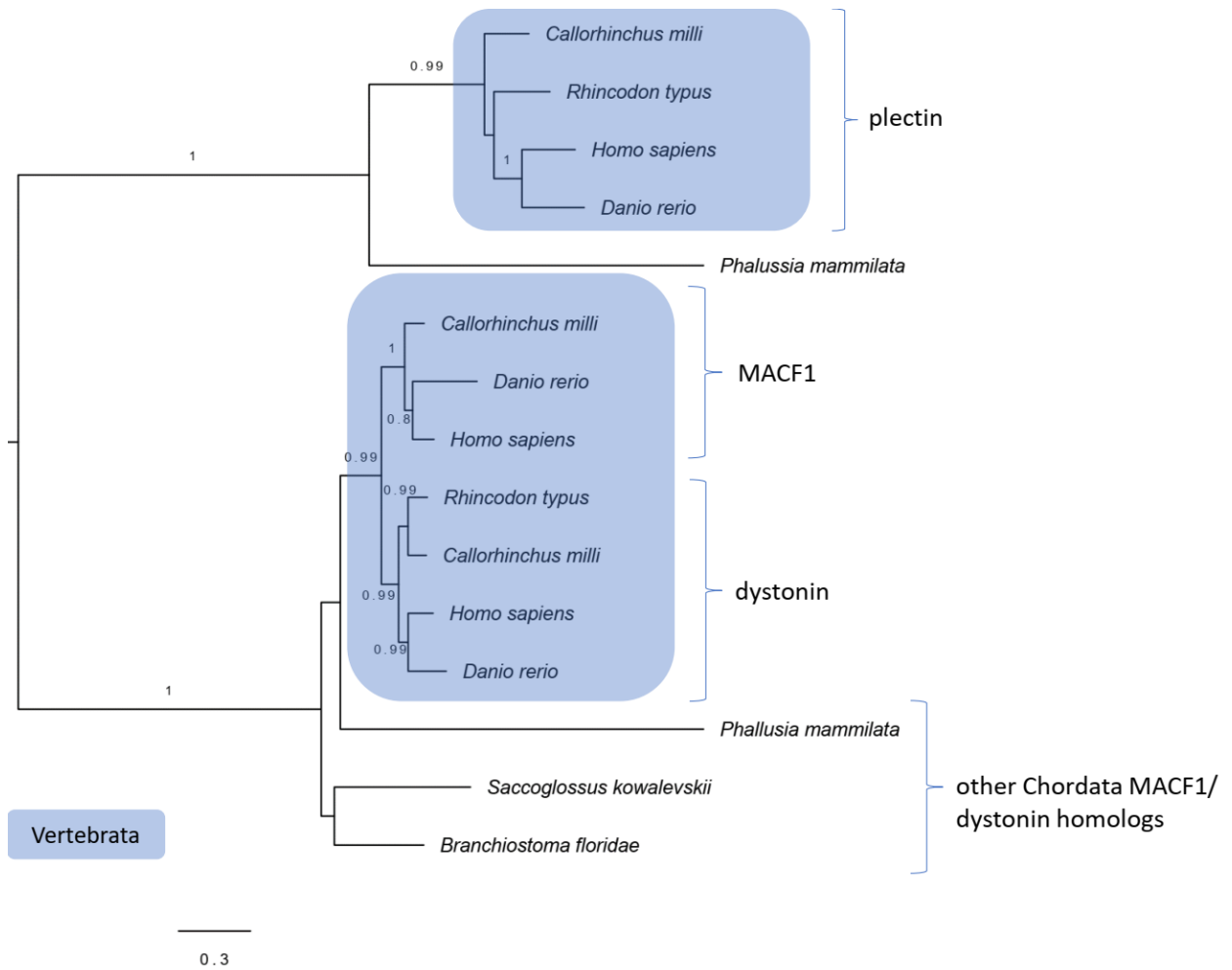


**Figure S3. ML tree of Chordata spectraplakins (dystonin and MACF1) and plakin (plectin) proteins.** The best-fit model according to AIC criterion was LG+G+T. aLRT values > 0.7 are shown inferring branch support. Sequences IDs are listed in Supplementary Table 1.

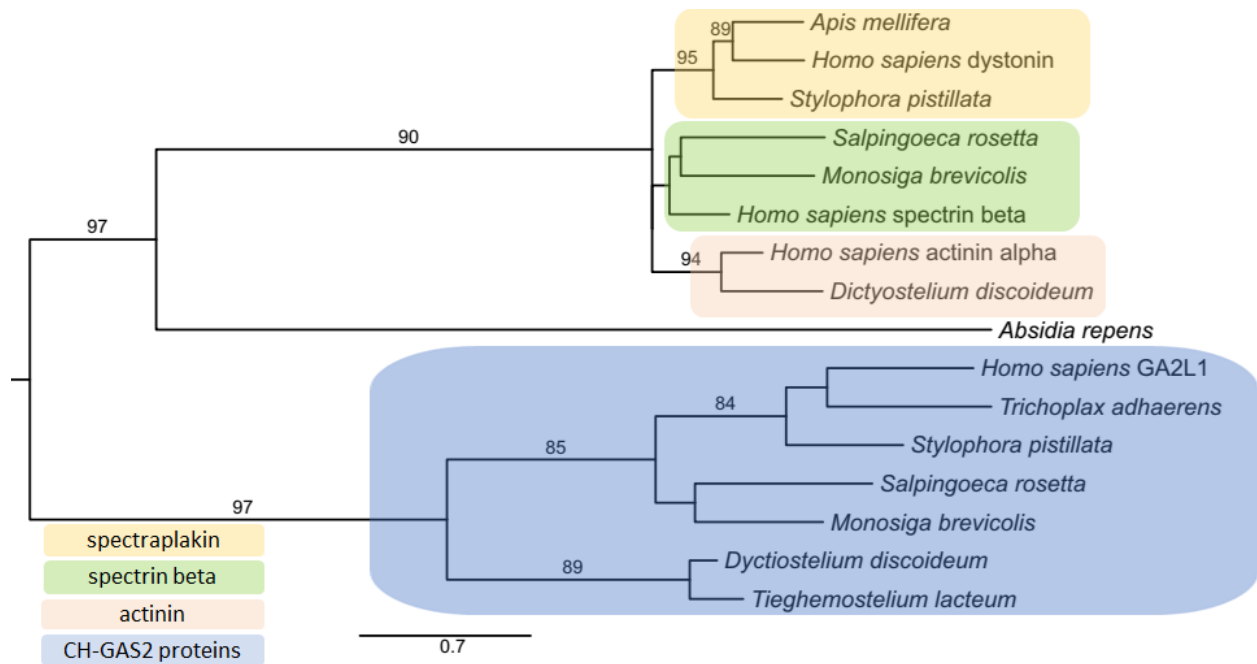


**Figure S4.** Phylogenetic relationship of CH domains that are present in different spectrins, spectraplakins and GAS2 proteins. The phylogenetic tree was reconstructed based on MSA of the CH domain using a maximum likelihood method. The best-fit model according to BIC criterion was LG+G4. Branch support is presented with UFBoot values (1000 replicates). Only >80 values are shown. The tree is midpoint rooted. IDs of sequences used to built the tree are indicated in the Supplementary Table 1.

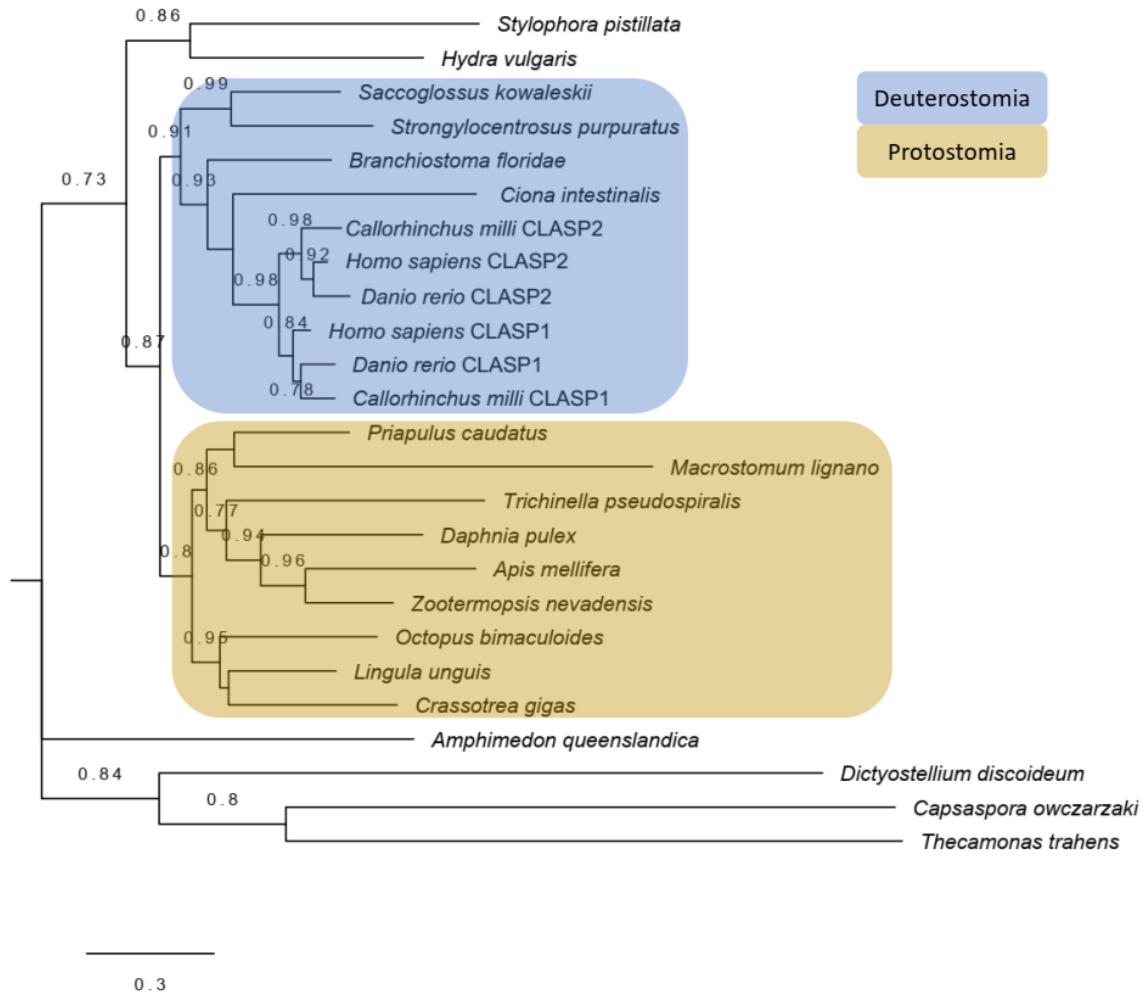


**Figure S5. ML tree of CLASP homologs in Opisthokonta and Apusomonada.**

The best-fit model according to AIC criterion was LG+G+I+F. aLRT values > 0.7 are shown to infer branch support. IDs of sequences used to build the tree: **Ddi** Q55BD8, **Aqu** A0A1X7V8T9, **C.o.** A0A0D2WMS0, **Tth** A0A0L0DWT2, **Mli** A0A267FQM7, **Hvu** XP\_012553551.1, **Spi** A0A2B4SA59, **Zne** A0A067R2S2, **Dpu** E9HJY5, **Ame** A0A7M7M181, **Tps** A0A0V0XXH6, **Pca** XP\_014663049, **Cgi** K1QCK4, **Lun** A0A1S3HCG9, **Obi** A0A0L8GA74, **Cin** F6W6K9, **Bfl** XP\_035658510.1, **Spu** A0A7M7N026, **Sko** XP\_006818149, **Hsa** CLASP1 Q7Z460, CLASP2 O75122, **Cmi** CLASP1 A0A4W3IJN8, CLASP2 A0A4W3JU88, **Dre** CLASP1 F1R253, CLASP2 F1R161.

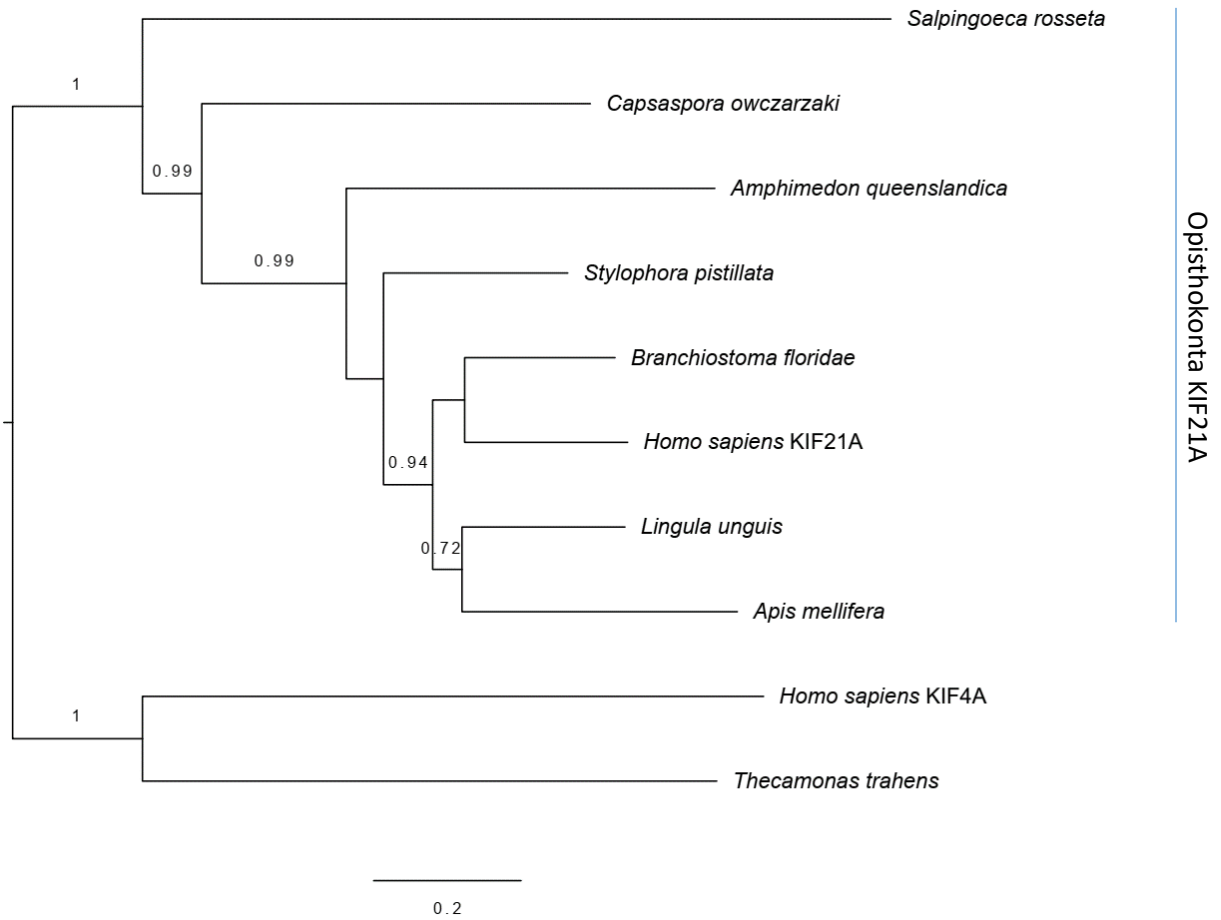


**Figure S6. ML tree of KIF21A homologs in Opisthokonta.** The best-fit model according to AIC criterion was LG+G+I+F. Closest KIF21A homolog from *T.trahens* (Apusomonada) is branching with human KIF4A. aLRT values > 0.7 are shown to infer branch support. IDs of sequences used to build the tree: **Hsa** KIF4A O95239, KIF21A Q7Z4S6, **Tth** A0A0L0DLG6, **Cow** A0A0D2VM81, **Sro** F2U9D0, **Aqu** A0A1X7UVT9, **Spi** A0A2B4S5K6, **Ame** A0A7M7GPK1, **Lun.** XP\_013396200.1, **Bfl** XP\_035660431.1.

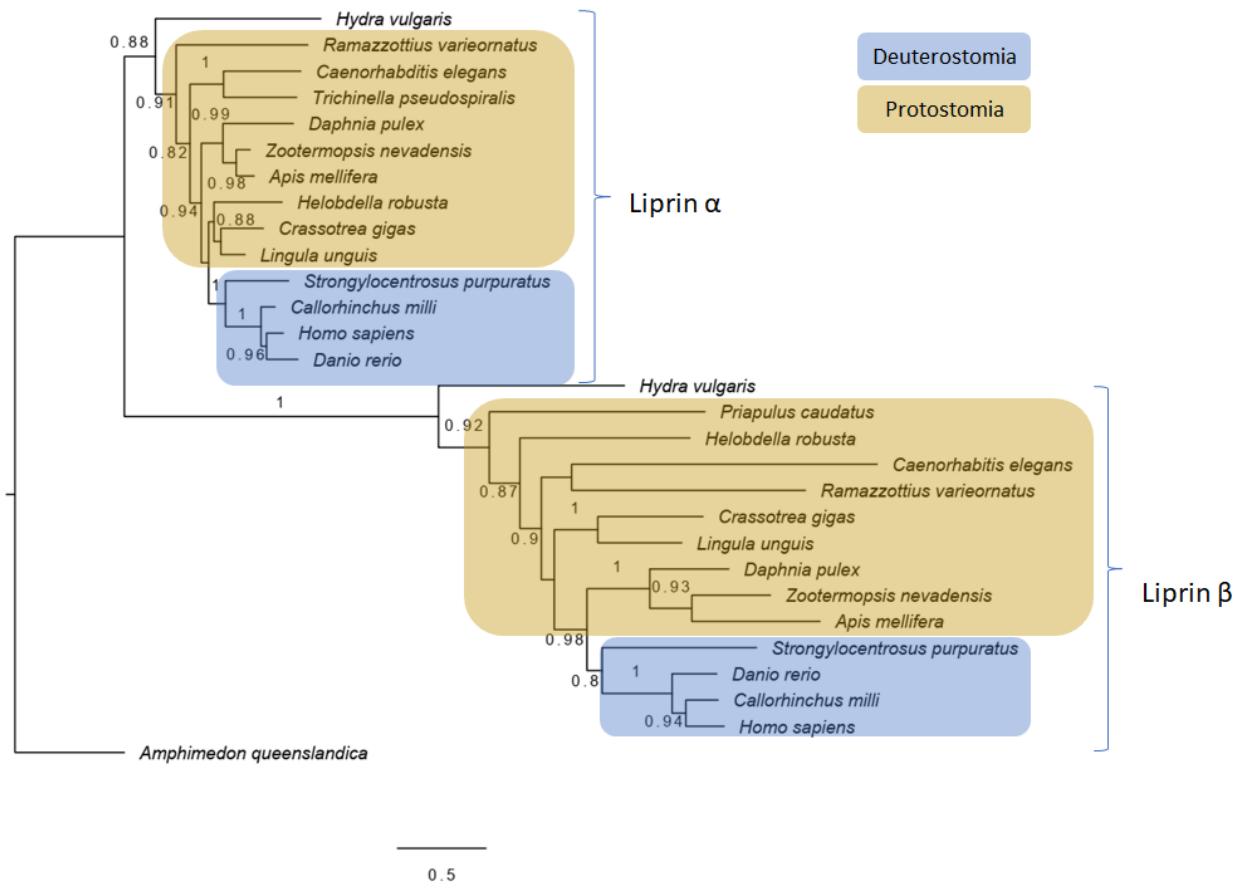


**Figure S7. ML tree of liprin homologs in Metazoa.** Eumetazoa species have both liprin  $\alpha$  and liprin  $\beta$  homologs, while *A.queenslandica* (Porifera) has single predicted liprin protein.

The best-fit model according to AIC criterion was LG+G+I+F. aLRT values > 0.7 are shown to infer branch support. IDs of sequences used to build the tree: **Aqu** A0A1X7V6S1; **liprin  $\alpha$** : **Hvu** XP\_004206607.1, **Rva** A0A1D1W4G4, **Cel** Q21049, **Tps** A0A0V0YF80, **Hro** T1FRP9, **Cgi** K1R1P0, **Lun** A0A1S3KA15, **Ame** A0A7M7MU22, **Dpu** E9FRQ5, **Zne** A0A067RU54, **Spu** A0A7M7P265, **Hsa** Q13136, **Dre** A9JR75, **Cmi** A0A4W3JHY5; **liprin  $\beta$** : **Hvu** XP\_012556355.1, **Pca** XP\_014673509.1, **Hro** T1EGH9, **Rva** A0A1D1V8S0, **Cel** Q94071, **Cgi** K1PZJ9, **Lun** A0A1S3JF91, **Zne** A0A067REV5, **Dpu** E9GYB0, **Ame** A0A7M7L1J8, **Spu** A0A7M7P464, **Hsa** Q86W92, **Dre** B7ZVC4, **Cmi** A0A4W3IRG3.

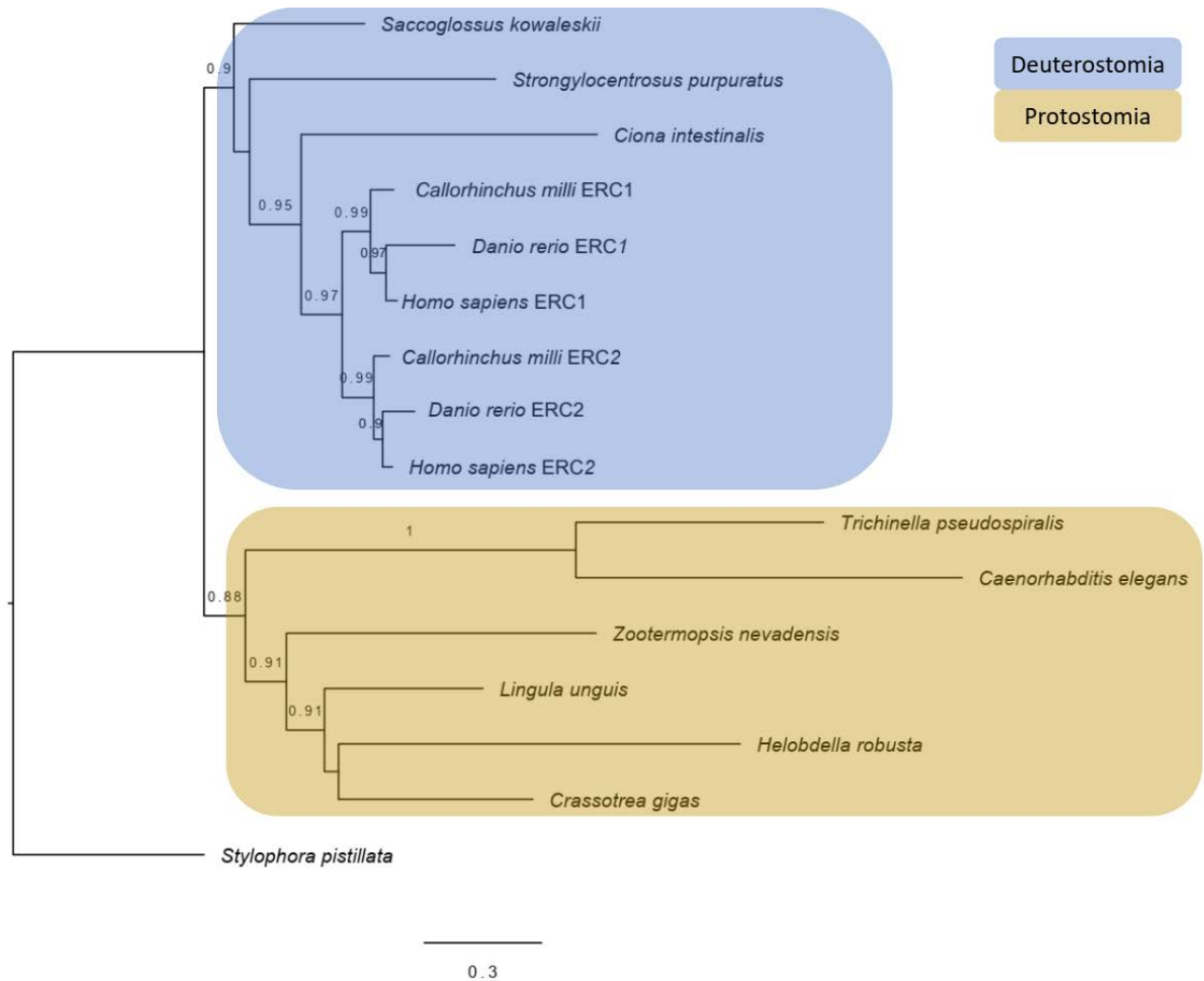


**Figure S8. ML tree of ERC homologs in Metazoa.** The best-fit model according to AIC criterion was JTT+G+I+F. aLRT values > 0.7 are shown to infer branch support. IDs of sequences used to build the tree: **Spi** A0A2B4SSH7, **Tps** A0A0V0XLN2, **Cel** O44490, **Cin** F6SDZ0, **Cmi** ERC1 A0A4W3K904, ERC2 A0A4W3GYW2, **Dre** ERC1 B7ZVS4, ELKS2 A0A0R4IGY4, **Hsa** ERC1 Q8IUD2, ERC2 O15083, **Spu** A0A7M7MX96, **Sko** XP\_006817071.1, **Hro** T1FWH3, **Lun** A0A1S3HA77, **Cgi** K1QCT1, **Pca** XP\_014676835.1, **Rva** A0A1D1UTD1, **Ame** A0A7M7LQU9, **Zne** A0A067QWS7.

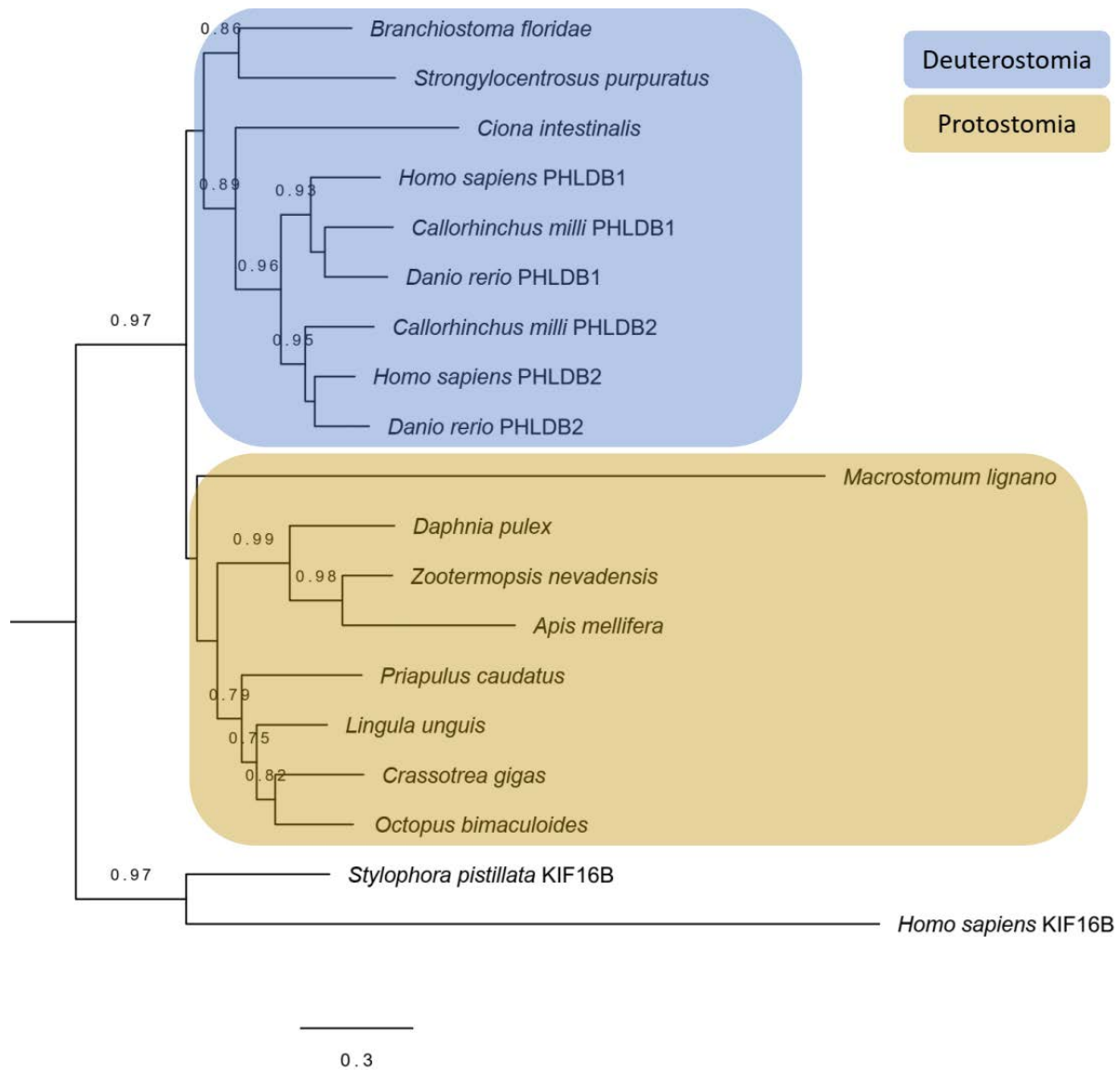


**Figure S9. ML tree of PHLDB homologs in Bilateria.** PHLDB homolog from *S.pistillata* (Cnidaria) is more closely related to *H.sapiens* KIF16B. The best-fit model according to AIC criterion was LG+G. aLRT values > 0.7 are shown to infer branch support. IDs of sequences used to build the tree: **Hsa** PHLDB2 Q86SQ0, PHLDB1 Q86UU1, KIF16B Q96L93, **Cmi** PHLDB1 A0A4W3GZF7, PHLDB2 UPI001C3F7021, **Dre.** PHLDB1 A2BFP0, PHLDB2 A0A0R4IA44, **Cin** F6PV66, **Bfl** C3XRU4, **Spu** A0A7M7NB47, **Dpu** E9G6U6, **Ame** A0A7M7L0H7, **Zne** A0A067QIX4, **Mli.** A0A267GFC2, **Lun** A0A1S3JKI4, **Pca** XP\_014665519, **Obi** UPI00071CB49E, **Cgi** K1RLW8, **Spi** A0A2B4SY28.

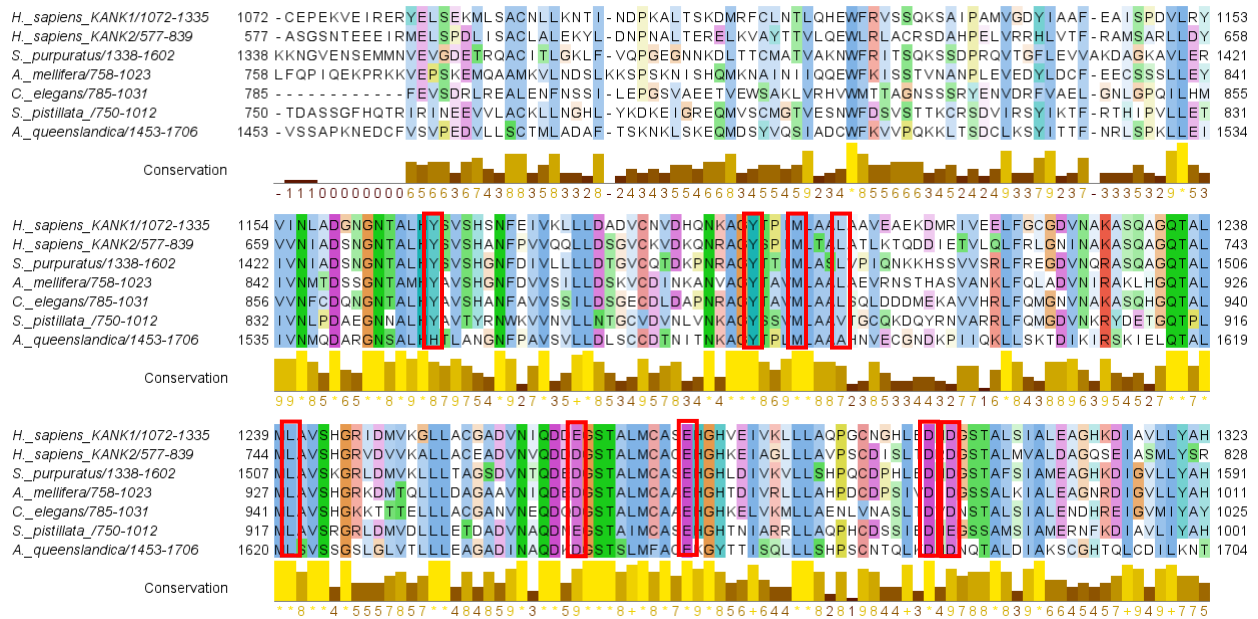


**Figure S10. Multiple sequence alignment of ankyrin domain of KANK proteins from different animals.** KIF21A binding residues are indicated by red boxes. Overall amino acid residues conservation is indicated below alignment; 0→\* increasing conservation. IDs of sequences used for the alignment: **Hsa** KANK1 Q14678, KANK2 Q63ZY3, **Spu** A0A7M7PJC8, **Ame** A0A7M7GUR2, **Cel** G5EDN8, **Spy** A0A2B4S5K6, **Aqu** A0A1X7UFY5.